

Prediction of the intestinal resistome by a three-dimensional structure-based method

Ruppé, Etienne; Ghozlane, Amine; Tap, Julien; Pons, Nicolas; Alvarez, Anne-Sophie; Maziers, Nicolas; Cuesta, Trinidad; Hernando-Amado, Sara; Clares, Irene; Martínez, Jose Luís; Coque, Teresa M; Baquero, Fernando; Lanza, Val F; Máiz, Luis; Goulenok, Tiphaine; de Lastours, Victoire; Amor, Nawal; Fantin, Bruno; Wieder, Ingrid; Andremont, Antoine

DOI:

[10.1101/196014](https://doi.org/10.1101/196014)

[10.1038/s41564-018-0292-6](https://doi.org/10.1038/s41564-018-0292-6)

License:

None: All rights reserved

Document Version

Peer reviewed version

Citation for published version (Harvard):

Ruppé, E, Ghozlane, A, Tap, J, Pons, N, Alvarez, A-S, Maziers, N, Cuesta, T, Hernando-Amado, S, Clares, I, Martínez, JL, Coque, TM, Baquero, F, Lanza, VF, Máiz, L, Goulenok, T, de Lastours, V, Amor, N, Fantin, B, Wieder, I, Andremont, A, van Schaik, W, Rogers, M, Zhang, X, Willems, RJL, de Brevin, AG, Batto, J-M, Blottière, HM, Léonard, P, Léjard, V, Letur, A, Levenez, F, Weiszner, K, Haimet, F, Doré, J, Kennedy, SP & Ehrlich, SD 2019, 'Prediction of the intestinal resistome by a three-dimensional structure-based method', *Nature Microbiology*, vol. 4, no. 1, pp. 112-123. <https://doi.org/10.1101/196014>, <https://doi.org/10.1038/s41564-018-0292-6>

[Link to publication on Research at Birmingham portal](#)

Publisher Rights Statement:

This is an author-produced, peer-reviewed version of an article published in *Nature Microbiology*, volume 4, pp.112–123 (2019), <https://doi.org/10.1038/s41564-018-0292-6>

General rights

Unless a licence is specified above, all rights (including copyright and moral rights) in this document are retained by the authors and/or the copyright holders. The express permission of the copyright holder must be obtained for any use of this material other than for purposes permitted by law.

- Users may freely distribute the URL that is used to identify this publication.
- Users may download and/or print one copy of the publication from the University of Birmingham research portal for the purpose of private study or non-commercial research.
- User may use extracts from the document in line with the concept of 'fair dealing' under the Copyright, Designs and Patents Act 1988 (?)
- Users may not further distribute the material nor use it for the purposes of commercial gain.

Where a licence is displayed above, please note the terms and conditions of the licence govern your use of this document.

When citing, please reference the published version.

Take down policy

While the University of Birmingham exercises care and attention in making items available there are rare occasions when an item has been uploaded in error or has been deemed to be commercially or otherwise sensitive.

If you believe that this is the case for this document, please contact UBIRA@lists.bham.ac.uk providing details and we will remove access to the work immediately and investigate.

1 **Prediction of the intestinal resistome by a 3D structure-based method**

2 Etienne Ruppé* (1, 2), Amine Ghozlane* (1, 3, 4) Julien Tap*§ (1), Nicolas Pons (1), Anne-Sophie
3 Alvarez (1), Nicolas Maziers (1), Trinidad Cuesta (5), Sara Hernando-Amado (5), Irene Clares (5), Jose
4 Luís Martínez (5), Teresa M. Coque (6, 7, 8), Fernando Baquero (6, 7, 8), Val F. Lanza (6, 7), Luis Maiz
5 (9), Tiphaine Goulenok (10), Victoire de Lastours (2, 10), Nawal Amor (10), Bruno Fantin (2, 10), Ingrid
6 Wieder (11), Antoine Andremont (2, 11), Willem van Schaik (12, 13), Malbert Rogers (12), Xinglin Zhang
7 (12), Rob J.L. Willems (12), Alexandre G. de Brevern (14), Jean-Michel Batto (1), Hervé M. Blottière (1),
8 Pierre Léonard (1), Véronique Lédard (1), Aline Letur (1), Florence Levenez (1), Kevin Weiszer (1),
9 Florence Haimet (1), Joël Doré (1), Sean P. Kennedy (1, 4), S. Dusko Ehrlich (1, 15)

10

11 (1) MGP MetaGénoPolis, INRA, Université Paris-Saclay, 78350 Jouy en Josas, France

12 (2) IAME, UMR 1137, INSERM, Paris Diderot University, Sorbonne Paris Cité,

13 (3) Bioinformatics and Biostatistics Hub, C3BI, Institut Pasteur, USR 3756 IP CNRS, Paris, France.

14 (4) Biomics, CITECH, Institut Pasteur, Paris, France.

15 (5) Centro Nacional de Biotecnología, CSIC, Madrid, Spain.

16 (6) Servicio de Microbiología. Instituto, Ramón y Cajal de Investigación Sanitaria (IRYCIS), Madrid,
17 Spain

18 (7) CIBER en Epidemiología y Salud Pública (CIBER-ESP), Madrid, Spain

19 (8) Unidad de Resistencia a Antibióticos y Virulencia Bacteriana (RYC-CSIC), Madrid, Spain.

20 (9) Unit for Cystic Fibrosis, Ramon y Cajal University Hospital, Madrid, Spain

21 (10) Internal Medicine Department, Beaujon Hospital, AP-HP, Clichy, France

22 (11) Bacteriology Laboratory, Bichat-Claude Bernard Hospital, AP-HP, Paris, France

23 (12) Department of Medical Microbiology, University Medical Center Utrecht, Utrecht, the Netherlands

24 (13) Institute of Microbiology and Infection, University of Birmingham, Edgbaston, Birmingham B15 2TT,
25 United Kingdom

26 (14) INSERM UMR_S 1134, Paris Diderot University, Sorbonne Paris Cité, Université de la
27 Réunion, Université des Antilles, INTS, GR-Ex, Paris, France

28 (15) Centre of Host Microbiome Interactions, King's college, London, United Kingdom

29

30 *The authors equally contributed to the study

31

32 § Current affiliation: Danone Nutricia Research, Palaiseau – France

33

34 **Corresponding author**

35 Etienne RUPPE (PharmD, PhD)

36 Laboratoire de Bactériologie

37 Hôpital Bichat-Claude Bernard

38 46 rue Henri Huchard

39 75018 Paris

40 France

41 Phone: +33(0) 1 40 25 85 04

42 Fax: +33(0) 1 40 25 85 81

43 etienne.ruppe@inserm.fr

44

45 **Opening paragraph**

46 The intestinal microbiota is considered to be a major reservoir of antibiotic resistance determinants
47 (ARDs) that could potentially be transferred to bacterial pathogens via mobile genetic elements (MGEs).
48 Yet, this assumption is poorly supported by empirical evidence due to the distant homologies between
49 known ARDs (mostly from culturable bacteria) and ARDs from the intestinal microbiota. Consequently,
50 an accurate census of intestinal ARDs (*i.e.* the intestinal resistome) has not yet been fully determined.
51 For this purpose, we developed and validated an annotation method (called pairwise comparative
52 modelling, PCM) based on 3D structure (homology comparative modelling) leading to the prediction of
53 6,095 ARDs in a catalogue of 3.9 million proteins from the human intestinal microbiota. We found that
54 the majority of predicted ARDs (pdARDs) were distantly related to known ARDs (mean amino acid
55 identity 29.8%) and found evidence supporting their transfer between species. According to the
56 composition of their resistome, we were able to cluster subjects from the MetaHIT cohort (n=663) into 6
57 “resistotypes” that were connected to the previously described enterotypes. Finally, we found that the
58 relative abundance of pdARDs was positively associated with gene richness, but not when subjects
59 were exposed to antibiotics. Altogether, our results indicate that the majority of intestinal microbiota
60 ARDs can be considered as intrinsic to the dominant commensal microbiota and that these genes are
61 rarely shared with bacterial pathogens.

62

63

64 **Introduction**

65 Antimicrobial resistance is one of the major threats to health identified by the World Health Organization
66 for the next decades. The intestinal microbiota plays a pivotal role in this phenomenon as it harbours a
67 vast diversity of bacterial species, some of them possessing antibiotic resistance determinants (ARDs)
68 that may enable their survival under antibiotic exposure. Previous studies attempted to identify ARDs in
69 the intestinal microbiota²⁻⁴ but were confounded by the distant homologies between known ARDs
70 (mostly from culturable bacteria) and ARDs from the intestinal microbiota (which are generally not
71 cultured)^{5,6}. For these reasons, bioinformatic tools based on sequence comparison (ARG-ANNOT⁷,
72 CARD – RGI⁸, Resfinder⁹, DeepARG¹⁰) or motif detection (Resfams¹¹) are often unsuccessful in
73 characterising the diversity of ARDs from metagenomic datasets. Indeed, there is no consensus on an
74 optimal approach to detect ARDs in metagenomic datasets. Consequently, an accurate census of
75 intestinal ARDs (*i.e.* the intestinal resistome) has not yet been fully determined.

76 While many bacteria have intrinsic, chromosomally-encoded ARDs and the capability of increasing
77 resistance through mutation, they can also enrich their resistance capabilities through the acquisition of
78 exogenous ARDs located on mobile genetic elements (MGEs) such as plasmids, transposons or
79 phages. The intestinal microbiota harbours thousands of bacterial species including well-known
80 pathogens (*e.g.* *Enterobacteriaceae* and *Enterococcus spp.*). This unique environment is assumed to
81 be a reservoir of ARDs that can potentially be transferred to bacterial pathogens¹³. Nonetheless despite
82 the high selective pressure exerted on the intestinal microbiota by over seven decades of intensive
83 antibiotic usage, a very low number of transfer events from an intestinal commensal to a bacterial
84 pathogen have been observed^{14,15}. This challenges the hypothesis of a mobile resistome and the
85 assumption that the intestinal microbiota serves as a reservoir of ARDs to which pathogenic bacteria
86 have easy access¹⁶. In this study, our objective was to perform an extensive characterization of the
87 human gut resistome (including the capacity of ARDs to transfer between species) and to assess its
88 dynamics under various antibiotic exposures.

89

90 **Prediction of ARDs in the intestinal microbiota**

91 To predict ARDs in the intestinal microbiota, we developed a method based on protein homology
92 modelling (see methods) that we termed PCM (for “pairwise comparative modelling”). PCM is a generic
93 method using homology modelling to increase the specificity of functional prediction of proteins,

94 especially when they are distantly related to potential homologs. PCM uses a list of reference proteins
95 sequences from a given family, the ARD structures of this family (used as structural templates in protein
96 data bank [PDB] format) and a series of negative references (Figure 1A, Supplementary Figure 1, 2 and
97 3). Structural models are built using both the ARD reference and negative reference templates. Scores
98 generated from both positive and negative references are used to determine which model performed
99 the best. This is done using a machine-learning algorithm trained on 662 ARD and 522 negative
100 references. The PCM score equals the number of times the query was classified as an ARD for the
101 bootstraps performed, expressed as a percentage. Candidates with a PCM score $\geq 50\%$ and an
102 alignment score with the reference template (TM score given by TM-align) $\geq 0.5^{17}$ were predicted as
103 ARDs.

104 The performance of PCM to predict ARDs was assessed using *in vitro* and *in silico* methods. We
105 synthesized 71 candidate ARDs from 12 families (Table 1), and expressed them in *Escherichia coli* (see
106 methods). All 12 pdARDs sharing an amino acid identity $>95\%$ with a known ARDs had a detectable
107 resistance activity against antibiotics (Figure 1B). Resistance activity was also detected in 35/41 (85.3%)
108 of the predictions made with a good level of confidence (PCM score $>99\%$, Tm score TmAlign >0.9) and
109 in 8/18 (44.4%) of the predictions with a lower level of confidence (PCM score $<80\%$, Tm score
110 TmAlign <0.8). The mean amino acid identity of the functional pdARDs (good and fair predictions, $n=43$)
111 with known ARDs was 28.6% (range 19.4%-82.6%, Supplementary Table 1). We then tested PCM
112 against an experimentally-validated functional metagenomics dataset from soils¹⁸. In this case, PCM
113 was able to accurately identify 1,374 ARDs out of 1,423 hits (sensitivity 96.6%) (see methods). Finally,
114 we assessed the performances of PCM with incomplete proteins as inputs, and showed that PCM could
115 correctly predict ARDs when the available amino acid sequence was at least 40% complete
116 (Supplementary Figure 4). After the *in vitro* and *in silico* validation of the method, we used PCM to search
117 for ARDs in the in a catalogue made of 3,871,657 proteins which was built from the sequencing of faecal
118 samples of 396 human individuals (177 Danes and 219 Spanish) recruited in the MetaHIT project¹⁹. In
119 total, we predicted 6,095 ARDs (0.2% of the catalogue) from 20 ARD classes conferring resistance to
120 nine major antibiotic families²⁰: beta-lactams (class A, B1-B2, B3, C and D beta-lactamases),
121 aminoglycosides (AAC(2'), AAC(3)-I, AAC(3)-II, AAC(6)'), ANT, APH, RNA methylases), tetracyclines
122 (Tet(M), Tet(X)), quinolones (Qnr), sulphonamides (Sul), trimethoprim (DfrA), fosfomycin (Fos) and
123 glycopeptides (Van ligases) (Table 1 and Supplementary Table 1). With the same, extensively curated

124 reference ARDs census as input, only 67 ARDs would have been predicted according to conventional
125 BLASTP²¹ search with a specific identity threshold (80% over 80% of the reference sequence)^{3,4}. ARG-
126 ANNOT⁷, Resfinder⁹ and DeepARG¹⁰ were able to predict 54, 50 and 2,139 ARDs, respectively, while
127 Resfams¹¹ predicted a very high number of ARDs (44,105). The HMM-based search for class B1 beta-
128 lactamases published by Berglund *et al.*²² also yielded a high number of hits (n=3,490) in the 3.9 million
129 protein catalogue (Figure 1C, Supplementary Figure 5). Further analysis on a catalogue of dummy,
130 synthetic 3.9 million proteins indeed showed that Resfams, DeepARG and the Berglund *et al.* HMM-
131 based search lacked specificity (see Supplementary Information). The mean identity shared between
132 predicted (n=6,095) and reference ARDs was 29.8%; it was significantly higher than candidates not
133 predicted as ARDs (mean 23.0%, Wilcoxon unpaired test p=2e-16, Figure 1D). Indeed, most of the
134 pdARDs were distantly related to reference ARDs (Supplementary Figure 6 and 7). Besides, PCM failed
135 to predict 16 ARDs which shared at least 40% identity with a reference ARD (Supplementary Table 2).
136 The 6,095 pdARDs and their structures are available at <http://mgps.eu/Mustard>.

137

138 **Taxonomic distribution of ARDs**

139 A host bacterial phylum could be assigned to 72.3% (4405/6095) pdARDs. The majority was identified
140 as from the dominant human intestinal phyla Firmicutes (2962/4405, 72.3%) and Bacteroidetes
141 (858/4405, 19.5%) (Supplementary Figure 8) with only 5.8% (225/4405) of pdARDs coming from
142 Proteobacteria. An additional seven pdARDs were predicted to be harboured by Archaea
143 (*Methanobrevibacter* and *Methanoculleus* genera), putatively conferring resistance to macrolides,
144 tetracyclines, aminoglycosides, sulphonamides and glycopeptides (Supplementary Table 1). We also
145 predicted ARDs in genera of medical interest where no ARDs had been identified such as *Akkermansia*²³
146 (10 pdARDs) and *Faecalibacterium*²⁴ (44 pdARDs). Only 23 out of 6,095 (0.4%) had been previously
147 identified in families and genera that include human pathogens (Enterobacteriaceae, *Campylobacter*,
148 *Enterococcus*, *Streptococcus* and *Acinetobacter*). The distribution of the families of pdARDs differed
149 according to the phyla (Supplementary Figure 9): Firmicutes and Proteobacteria were enriched with
150 aminoglycosides-modifying enzymes (AMEs, spanning APH, ANT, and AACs) whereas Bacteroidetes
151 were enriched in Sul and class A beta-lactamases. Interestingly, the tigecycline-degrading
152 monooxygenase Tet(X) was frequently found in Bacteroidetes and Proteobacteria, the two phyla
153 between which transfer of the *tet(X)* gene has been reported^{14,25}. In order to support these assignments,

154 we sequenced the metagenome of four human faecal samples before and after an overnight culturing
155 using conditions that favoured the growth of oxygen-tolerant bacteria such as Enterobacteriaceae and
156 enterococci (see methods). The results showed an enrichment of Proteobacteria (over Firmicutes and
157 Bacteroidetes), and a commensurate increase of class C beta-lactamases, Fos and Tet(X), along with
158 Van ligases (Supplementary Figure 10).

159

160 **Location of the pdARDs and association with mobile genetic elements**

161 We investigated the potential for mobility of the pdARDs at different levels. First, we took advantage of
162 the identification of gene clusters based on co-abundance and co-occurrences of genes among the 396
163 faecal metagenomes used to build the 3.9 million MetaHIT gene catalogue¹⁹. A total of 7,381 gene
164 clusters referred to as metagenomic units (MGUs) were identified. Among MGUs, metagenomic species
165 (MGS) are defined as MGUs with ≥ 700 genes, which are considered to be representative of partial or
166 complete bacterial genomes¹⁹. MGUs of < 700 genes include MGEs such as plasmids, phages,
167 transposable elements, and incomplete chromosomal sequences. The 7,381 MGUs from the 3.9 million
168 gene catalogue of intestinal microbiota gene were queried with the pdARDs. A total of 3,651 (59.9%)
169 pdARDs could be mapped onto an MGU. The distribution of pdARDs as a function of MGU size is shown
170 in Figure 2A. Most (95.6%, 3,489/3,651) pdARDs mapped onto MGS and the relative abundance of
171 pdARDs correlated strongly with the abundance of their respective MGS (Supplementary Information),
172 supporting their location on the same bacterial host across the 396 individuals. We also searched for
173 pdARDs in metagenomic species pan-genomes (MSPs)²⁶ obtained from the 9.9 million intestinal gene
174 catalogue²⁷. Similar to MGS, MSPs are clusters of genes that are co-abundant in a set of sample. In
175 MSPs, genes that are constantly found are referred as “core” while inconsistently found genes are
176 referred to as “accessory”. Besides, “shared core” genes are assumed to be conserved genes shared
177 between phylogroups²⁶. We found 4,912 pdARDs located on MSPs, with the majority being assigned to
178 the core pangenome (4,099/4,912, 83.4%) or shared between core-pangenomes (389/4,912, 7.9%).
179 This was different with MGE-associated genes²⁷ with most being not found in MSPs (Figure 2B).
180 Then, we investigated whether genes associated with gene mobility (transposases, conjugative
181 elements and integrons) were present on the same contig than the pdARDs. We found that 7.9%
182 (484/6,095) of pdARDs were co-located with homologs of MGE-associated genes. For pdARDs not

183 found in MGS or in MSPs (n=974), 876 (89.9%) had no detectable MGE-associated genes in their
184 vicinity.

185 Finally, we searched for pdARDs homologs (BLASTN >97% identity over >90% of the query length) in
186 the Genbank database (2018 July 11). Only 538 pdARDs homologs were identified, with 49 being
187 located on a plasmid and/or a phage (Supplementary Table 3). Among the 489 remaining pdARDs, 82
188 (16.8%) were found in multiple species, mainly (60/82, 73.2%) from the same genus (Supplementary
189 Table 4).

190 The phyla Bacteroidetes, Firmicutes and Tenericutes had the higher proportions of ARDs co-locating
191 with MGEs (Figure 2C). No ARD family was found to be enriched in MGE, with the exception of the
192 Tet(X) family in which 3 out of 9 (33.3%) predictions (2 from *Bacteroides fragilis* and 1 from *E. coli*) were
193 associated with transposases (Figure 2D).

194

195 **Distribution of pdARDs in human hosts' microbiota**

196 In the MetaHIT cohort (663 subjects), we found that subjects carried pdARDs with a median relative
197 abundance of 0.22% (range 0.14%-0.38%), with pdARDs from the Tet(M) family being the most
198 abundant (0.07%) and those from class B3 beta-lactamases the least (median: 0.004%). The average
199 number of unique pdARDs genes detected per metagenome was 1,377 (range 258-2,367). Most
200 pdARDs were shared across multiple subjects, 987/6,095 (16.2%) were found in at least 50% of
201 individuals, and only 106/6,095 (1.7%) occurred uniquely in a single individual. All ARD families, with
202 the exception of RNA methylases and AAC(2') families, were found in more than 80% of individuals.

203 Then, we assessed whether subjects with no recent exposure to antibiotics could cluster according to
204 their intestinal resistome. Based on the pdARDs family patterns, six clusters (that we named
205 "resistotypes" by analogy with the enterotypes²⁸) were detected using Dirichlet multinomial mixture
206 models (Supplementary Figure 11). The four most frequent resistotypes each represented around 20%
207 of the cohort (the fifth and the sixth representing 8.7% and 7.5%, respectively). The three first
208 resistotypes were characterized by a high abundance of Van ligases (Supplementary Figure 12).
209 Resistotype 1 was enriched in ANT, while resistotype 3 was driven by Tet(M) and class C beta-
210 lactamases. Resistotype 4 was enriched with Tet(X) and class A beta-lactamases and resistotype 6 in
211 class B1 beta-lactamases and Sul. We observed that resistotypes, as determined by PCM, were highly
212 connected to the composition of the microbiota, and that this effect was more pronounced than

213 resistotypes determined from the results of BLASTP and Resfams (Figure 3A). The resistotypes of the
214 MetaHIT cohort were found to be associated with enterotypes (chi square test, $p=5e-4$), Figure 3B-D,
215 Supplementary Figure 13). Resistotypes 1 and 3 had higher gene richness and were associated with
216 the Clostridiales–driven enterotype. Resistotype 4 was more prevalent in enterotypes driven by
217 *Bacteroides* (known to harbour Tet(X) and class A beta-lactamases) while resistotype 6 was very
218 specific to the *Prevotella* enterotype (Figure 3C-D). The relative abundance of pdARDs was observed
219 to be positively correlated to the gene richness (Figure 4A, Spearman's rank correlation test $Rho=0.31$,
220 $p=5e-16$). Conversely, we did not find any link between resistotypes and body mass index, age or
221 gender.

222

223 **Dynamics of the pdARDs under various exposures to antibiotics**

224 We investigated the abundances of pdARDs in subjects under various exposures to antibiotics and
225 healthcare environments. Three types of exposure were considered (see methods for details):
226 hospitalization in a French hospital without receiving antibiotics, $n=15$, chronic exposure (Spanish cystic
227 fibrosis patients frequently exposed to antibiotics, $n=30$) and short high-dose exposure through selective
228 digestive decontamination [SDD; oral colistin, tobramycin, antifungal amphotericin and parenteral
229 cefotaxime²⁹] at admission in intensive care units in Netherlands, $n=10$). We again confirmed a positive
230 correlation between relative abundance of pdARDs and gene richness among patients unexposed to
231 antibiotics (Figure 4B, Spearman's rank correlation test $Rho=0.37$, $p=0.01$, see methods). However,
232 when all the samples were considered, including those with antibiotic exposure, this relationship was no
233 longer present (Figure 4C). Instead, the relative abundance of pdARDs was found to be higher in
234 subjects with a chronic exposure than in subjects with no recent exposure (Figure 4D, Wilcoxon unpaired
235 test, $p=1e-10$), and gene richness was lower (Figure 4E, Wilcoxon unpaired test, $p=0.006$) In particular,
236 subjects with chronic exposure carried more class B1-B2 beta-lactamases, AAC(6'), ANT, APH, Erm,
237 and DfrA with lower abundance of Sul (Supplementary Figure 14). At the phylum level, we observed a
238 decrease of Bacteroidetes and Verrucomicrobia and an increase of Firmicutes and Actinobacteria in
239 patients chronically exposed to antibiotics (Supplementary Figure 15). A total of 74 MGS were found to
240 be differentially abundant among subjects with or without chronic exposure to antibiotics (Supplementary
241 Table 5).

242 This was different with subjects before and after SDD. A drastic loss of gene richness was measured
243 for this group (Figure 4E): from a mean of 295,919 genes to 95,286 (67.8 % reduction, Wilcoxon paired
244 test, $p=0.006$). Meanwhile, the relative abundance of pdARDs did not change significantly (Figure 4D,
245 $p=0.4$). At the ARD family level, we observed that some families decreased significantly: class C beta-
246 lactamases (commonly found in Enterobacteriaceae and Pseudomonadaceae which are specifically
247 targeted by SDD), Fos, Tet(X), APH and ANT (Supplementary Figure 16). We then analysed the MGS
248 at the phylum level and found that Proteobacteria, Actinobacteria, Firmicutes and Fusobacteria
249 decreased significantly after SDD (Supplementary Figure 17). A total of 358 MGS were found in this
250 cohort and, despite the small number of subjects ($n=10$), we found 133 MGS for which a significant
251 variation was observed (Supplementary Table 6). We tested whether a high abundance of pdARDs
252 could be protective against the antibiotics used in SDD, but found no association: the relative abundance
253 of pdARDs before SDD was not linked to the gene richness after SDD. Hospitalization without antibiotic
254 therapy, that is, potential exposure to antibiotic-resistant nosocomial pathogens without selective
255 pressure, did not affect the gene richness nor the relative abundance of pdARDs (Figure 4D and 4E).

256

257 **Discussion**

258 The results of this study support the concept that the majority of ARDs from the intestinal microbiota are
259 hosted by commensal bacteria, and that their transfer between species (including to opportunistic
260 pathogen) is rare³⁰. We provide several findings to support this assumption: 1) we used a 3D structure-
261 based method to assess the diversity of ARDs in the intestinal microbiota and confirmed that ARDs
262 predicted by PCM in the intestinal microbiota were distantly related to known ARDs, 2) the sensitivity
263 and the specificity of the method was validated by gene synthesis of a subset of predictions and by
264 benchmarking against various datasets (functional metagenomic of the soil microbiota, genomes and
265 random protein catalogues), 3) the majority of pdARDs could be found in clusters of co-abundant genes
266 (MGS and MSPs) in large cohorts of samples, while only a minority was found on plasmids, phages or
267 in the vicinity of MGE-associated genes, 4) we could stratify subjects into 'resistotypes' that were
268 connected to enterotypes, and 5) gene richness, otherwise associated with a healthy status³¹, was
269 positively correlated to the abundance of ARDs in subjects not exposed to antibiotics.

270 Our results challenge the paradigm that ARDs of the intestinal microbiota are a threat to public health.

271 As was previously demonstrated for environmental samples^{18,32}, ARDs tend to cluster according to the

272 underlying microbial ecology of the ecosystem, suggesting that the vast majority of ARDs are fixed in
273 their microbial hosts and are not, or very rarely, transferred. Our results show that the dominant intestinal
274 microbiota are not a major conduit through which opportunistic pathogens can acquire ARDs.
275 Nevertheless, we acknowledge that such transfer events have been reported^{14,15} and that
276 consequences for public health can be important, as in the case of the *vanB* vancomycin resistance
277 operon that is shared by *Clostridium* spp. and enterococci¹⁵. Understanding the mechanisms that can
278 lead to the mobilisation of ARDs in the intestinal microbiota, as well as a broader census of
279 environmental reservoirs of ARDs (e.g. sewage, livestock, the subdominant human intestinal
280 microbiota) will continue to be an important area for future research.

281 We found that subjects cluster according to the composition of their resistome into six groups that we
282 named “resistotypes” (as a reference to the previously described enterotypes²⁸). These resistotypes
283 were indeed connected to the enterotypes. Description of this underlying structure is interesting as one
284 might hypothesize that a particular resistotype, or microbiota enriched with ARDs, might be affected to
285 different degrees by antibiotic therapy. This has previously been observed for beta-lactamase-producing
286 *Bacteroides* which can protect the microbiome against exposure to β -lactams³³. In patients undergoing
287 faecal microbiota transplantation, follow-up antibiotic therapy may be adjusted to favour engraftment of
288 the donor microbiota³⁴. Identifying donors with a resilient microbiota, due to a protective resistotype,
289 could open perspectives for the optimisation of the clinical implementation of faecal microbiota
290 transplants.

291 Contrary to initial expectations, some pdARD families decreased in their abundance under antibiotic
292 exposure, especially when patients were exposed to a combination of antibiotics (such as SDD). In order
293 to resist to a combination of antibiotics, bacteria would need to be intrinsically resistant or to acquire an
294 adequate combination of ARDs. The dynamics of ARDs under antibiotic exposure depend on various
295 parameters: spectrum of the ARD (the level of resistance towards the antibiotic provided by the ARD),
296 the expression level of the ARD, and the presence of other resistance mechanisms (intrinsic or
297 acquired). The large number of possible combinations of these factors can explain that in some
298 situations, a bacterium can be inhibited by antibiotics despite the presence of a putatively compatible
299 ARD. Alternatively, we cannot exclude that changes in pdARDs families could also be explained by
300 simple taxonomic shifts that are not connected to the antibiotics studied.

301 The limitations of current techniques and of this study leave a number of important questions unresolved.
302 As mentioned earlier, metagenomic sequencing provides information for the dominant fraction of
303 intestinal bacteria, and so ARDs present in subdominant bacteria remain unobserved. Indeed, several
304 ARDs found in opportunistic pathogens among the Enterobacteriaceae (e.g. *Escherichia*
305 *coli* and *Klebsiella pneumoniae*) originate from other species in the same Proteobacteria phylum³⁵. A
306 recent study indeed cultured many Proteobacteria species that were not detected in metagenomic
307 sequencing³⁶. We cannot rule out that the subdominant bacteria, which were not probed by
308 metagenomic sequencing, could be an additional reservoir of ARDs. In terms of the clinical samples
309 analysed, we cannot exclude that the differences between patients and controls may be resulting from
310 confounding factors other than the antibiotic exposure.

311 The method we used to identify distantly related proteins is based on homology modelling and takes
312 advantage of the observation that proteins sharing the same function have more similar structures than
313 amino acid sequences³⁷. Indeed, PCM could identify functional ARDs with amino acid identity below
314 20% to known ARDs. Notably, PCM can only be used to predict the function of genes that are
315 homologous to known ARDs, and therefore the identification of different classes of ARDs with no
316 homology to known ARDs will still require functional screening. Besides, while PCM was validated in
317 this study, it remains a prediction tool. While similar structures are usually indicative of similar function,
318 this is not always the case and PCM can yield false positives results (as observed in the functional
319 validation of synthesized pdARDs). Due to the scope of our study, gene synthesis validation was not
320 performed for all ARD families, leaving open the possibility that not all pdARDs identified here truly have
321 a role in antibiotic resistance.

322 In summary, we developed a method, PCM, which could unveil the diversity of ARDs in the intestinal
323 microbiota. Employing this tool, we gathered evidence that the vast majority of the ARDs we predicted
324 showed no sign of mobility and that their abundance was correlated to gene richness. Together with the
325 protective trait of some intestinal bacteria against antibiotics³³, our results suggest that the ARDs from
326 the intestinal microbiota might be considered as our “resilience allies”³⁸ assuring the preservation of the
327 healthy commensal microbiota under antibiotic exposure.

328

329 **Acknowledgements**

330 The authors are deeply grateful to the GENOTOUL (Toulouse, France), GENOUEST (Rennes, France),
331 ABIMS (Roscoff, France), MIGALE (Jouy-en-Josas) and TGCC-GENCI (Institut Curie) calculation
332 clusters. The authors also warmly thank Bruno Perichon (Institut Pasteur, Paris, France) for providing
333 ARD sequences from *Acinetobacter baumannii*, Patricia Siguier (CNRS, Toulouse, France) for helping
334 the search of insertion sequences with ISfinder, Julien Guglielmini (Institut Pasteur, Paris, France) for
335 his assistance in finding conjugative elements, Stevonn Volant (Institut Pasteur, Paris, France) for the
336 design of the statistical model in SHAMAN, Thomas Jové (University of Limoges, France) for his
337 assistance in finding integrons, Marie Petitjean (IAME Reserch Center, Paris, France) for her assistance
338 in bioinformatic analyses, Florian Plaza-Oñate and Mathieu Almeida for their help with MSPs.

339

340

341 **Funding**

342 The project was funded in part by the European Union Seventh Framework Programme (FP7-HEALTH-
343 2011-single-stage) under grant agreement n° 282004, EvoTAR. IRYCIS authors acknowledge the
344 European Development Regional Fund “A way to achieve Europe” (ERDF) for co-founding the Spanish
345 R&D National Plan 2012-2019 Work (PI15-0512), CIBER (CIBERESP; CB06/02/0053), and the
346 Government of Madrid (InGeMICS- B2017/BMD-3691). Val F. Lanza was further funded by a Research
347 Award Grant 2016 of the European Society for Clinical Microbiology and Infectious Diseases (ESCMID).

348

349 **Conflicts of interest**

350 None.

351

352 **Authors' contribution**

353 ER, AG, JT performed the analysis. ER, AG, JT, WvS, AdB and SPK wrote the manuscript. ASA and
354 NM handled the data management. TC, SHA, IC and JLM performed the gene synthesis experiments.
355 JLM, TMC, VFL, FB, AdB, JD, SPK, FH and SDE discussed the protocol and results. LM, TG, VdL, NA,
356 BF, IW, AA, WvS, MR, XZ and RJL recruited the patients and collected the samples. HB, VL, AL and
357 FL handled the wet lab experiments. NP, PL and JMB managed the informatics and the calculation
358 clusters. KW and NP designed the website (<http://mgps.eu/Mustard/>).

359

360

361 **Methods**

362 **Constitution of the databases of antibiotic resistance determinants**

363 We define as an ARD as in Martinez *et al*⁸⁹: a protein encoded by a gene that confers resistance to
364 antibiotics when it is present or increases susceptibility to antibiotics when it is absent. This definition
365 excluded housekeeping genes in which mutations can confer resistance to some antibiotics (such as
366 topoisomerases in which mutations can lead to fluoroquinolone resistance) and genes involved in the
367 regulation of antibiotic resistance genes. Also, we excluded efflux pumps such as TetA or QepA as very
368 few or no PDB are available, presumably due to the difficulty to crystallize transmembrane proteins.
369 Amino acid sequences of functionally characterized ARDs from the major antibiotic families used in
370 human medicine (beta-lactams, aminoglycosides, tetracyclines, trimethoprim, sulfonamides,
371 macrolides-lincosamides-synergistines, fluoroquinolones, fosfomycin and glycopeptides)^{20,40} were
372 obtained from the following antibiotic resistance databases: Resfinder⁹, ARG-ANNOT⁷, the Lahey Clinic
373 (<http://www.lahey.org/studies/>), RED-DB (<http://www.fibim.unisi.it/REDDDB/>), Marilyn Roberts's website
374 for macrolides and tetracycline resistance genes (<http://faculty.washington.edu/marilynr/>) and from
375 functional metagenomics studies^{5,6,41}. When ARDs were provided as nucleic acids sequences, they
376 were translated into proteins with Prodigal⁴². Non-redundancy of the reference ARDs was assessed with
377 CD-HIT v4.5.7⁴³ (100% identity). The final database was manually curated in order to remove incomplete
378 sequences and ARDs from families not considered in this work. The cluster of orthologous genes (COG)
379 of each member of the reference dataset was assigned from the v3 eggNOG database⁴⁴. In total, we
380 collected 1,651 non-redundant amino acid sequences spanning 20 ARDs families: Class A beta-
381 lactamases (Blaa), class B1-B2 beta-lactamases (Blab1), class B3 beta-lactamases (Blab3), class C
382 beta-lactamases (Blac), class D beta-lactamases (Blad), aminoglycoside acetyltransferases (AAC)
383 AAC(2'), AAC(3)-I, AAC(3)-II, and AAC(6'), aminoglycoside nucleotidyltransferases (ANT),
384 aminoglycoside phosphotransferases (APH), 16S rRNA methylases, Tet(M), Tet(X), type A
385 dihydrofolate reductases (DfrA), dihydropteroate synthases (Sul), erythromycin ribosome methylases
386 (Erm), quinolone resistance proteins (Qnr), fosfomycin resistance proteins (Fos), and D-Ala – D-Lac/Ser
387 ligases (Van) (Table 1). The recently described plasmid-mediated colistin resistance *mcr-1* gene⁴⁵ could
388 not be included because of the lack of a reliable PDB template obtained by X-ray diffraction at the time
389 of the study.

390

391 **Interrogation of the catalogue for ARDs**

392 We used a 3,871,657 million proteins catalogue previously published¹⁹. This catalogue was built from
393 the metagenomic sequencing of the faeces of 396 subjects from Denmark and Spain. In brief, the 3.9
394 million gene catalogue results from a non-redundancy filtering at 95% nucleic acid identity and 90%
395 coverage: predicted genes from all samples (45.4 million in total) were clustered using BLAT by single
396 linkage. Any two genes with greater than 95% identity and covering more than 90% of the shorter gene
397 were clustered together. The contigs were originally built using SOAPdenovo (from the MOCAT
398 pipeline⁵²). We selected this catalogue over the more recent 10 million gene catalogue that was
399 published during the course of this study²⁷ because metagenomic units (MGUs, including the
400 metagenomic species [MGS]) had been determined only for the 3.9 million gene catalogue. The genes
401 of the catalogue were translated into proteins using Prodigal⁴² using the `-p meta` option. For each ARD
402 family, we searched for ARDs using the three following methods: (i) we built a hidden Markov model file
403 for each ARD family and searched the catalogue with Hmsearch (v3. 1)⁴⁶, (ii) we performed a Smith-
404 Waterman alignment with a heuristic seed detection (BLASTP v. 2. 2. 28+)²¹ and (iii) a rigorous Smith-
405 Waterman search (SSearch v. 36. 3. 6)⁴⁷ with an E-value threshold of 1E-5. Only the hits with a size
406 ranging from 75% and 125% of the mean amino acid size of the ARD family were further considered.
407 All candidates were assigned a COG/NOG from eggNOG v3⁴⁴. When candidates were found in different
408 ARD families (e.g. a candidate could be a hit in class B1-B2 and class B3 beta-lactamases), the
409 candidate was assigned to the family for which it had the highest amino acid identity with the reference.
410

411 **Negative references**

412 For each ARD family, COGs/NOGs were attributed to reference ARDs. In parallel, the COGs/NOGs
413 were attributed to the hits obtained during the initial steps of PCM (i.e. the hits obtained by the
414 BLASTP/SSearch and Hmmer search). In the list of candidates from a given ARD family, the
415 COGs/NOGs that were not found in the COGs/NOGs attributed to reference ARDs were assumed to be
416 potential COGs/NOGs from false positives hits (Supplementary Figure 2) as it reproduced the errors of
417 functional assignment likely to be generated in sequence-only annotations. The amino acid sequences
418 of the representative proteins from those COGs/NOG groups were obtained from the eggNOG v3
419 database, and were added to the negative reference dataset. A manual curation step was performed in
420 order to ensure that no references were included in the negative references.

421

422 **Selection of structural templates**

423 The list of protein structures that could be used as structural templates was downloaded (June 2014,
424 and November 2014) from the PDB library (Protein DataBank⁴⁸, <http://www.rcsb.org/>). Using the
425 reference dataset and the negative references described above, Hmmer⁴⁶, BLASTP²¹ and SSearch⁴⁷
426 were performed on the PDB database with default settings and E-values of 1E-5. Results were merged
427 into a non-redundant PDB list. Both lists (references and negative templates) were manually curated to
428 ensure that no references were represented in the negative templates dataset, and vice versa. If more
429 than one PDB shared the same UniProt number (i.e. if the structure of a protein has been determined
430 on multiple occasions), we filtered the PDB files in order to include a unique structure per UniProt number
431 using the following positive criteria: absence of ligand, completeness of the protein and high resolution.

432

433 **Pairwise comparative modelling**

434 The concept of pairwise comparative modelling (PCM) is shown in Supplementary Figure 1-3 and the
435 framework is available at <https://github.com/aghazlane/pcm>. The concept of
436 leveraging the protein structure in complement to its amino acid sequence was motivated by the fact
437 that proteins sharing common functions would be more conserved in the active site which cannot be
438 observed by the analysis of protein sequence alignments³⁷. Each candidate was subjected to homology
439 modelling with reference templates and negative templates, generating two 3D structures for each
440 candidate (Fig 1A). The main idea is that if a sequence is truly functionally related to the reference fold,
441 its model must be significantly different from the ones obtained with the negative structural template.
442 Homology modelling was performed by PCM in six main steps (example in Supplementary Figure 3):

- 443 1. Three structural templates were identified by BLASTP (among the lists produced as described
444 above) that shared the highest amino acid identity with the candidate protein.
- 445 2. A multiple sequence alignment was performed between the candidate and the three templates
446 sequences using Clustalo⁴⁹.
- 447 3. A prediction of the secondary structure was performed using psipred (v3.5)⁵⁰. The residues
448 predicted to fold in helix or in beta-sheet conformation with a level of confidence higher or equal to 7
449 were considered to constrain the model.

450 4. A comparative modelling was performed with the MODELLER programming interface⁵¹.
451 MODELLER automatically calculates a model by satisfaction of spatial restraints such as atomic
452 distance and dihedral angles in the target sequence, extracted from its alignment with the template
453 structures. Stereo-chemical restraints for residues are obtained from the CHARMM-22 molecular force
454 field and statistical preferences obtained from a representative set of known protein structures.

455 5. The best model out of a hundred produced by MODELLER (based on the Dope score) was
456 considered for structure assessment analysis using ProQ⁵² and Prosa-web⁵³. The Dope score
457 (Modeller), z-score (Prosa), MaxSub and LG score (ProQ) are statistical potential variables used to
458 predict the model quality. Both ProQ and Prosa-web are trained on the PDB to determine real protein
459 configuration and they estimate the energetic favourability of the conformation of each residue in the
460 model.

461 6. The best model was aligned with the reference set of structures using TM-align¹⁷ and
462 MAMMOTH⁵⁴. The RMSD (TM-align), z-score (MAMMOTH), TM-score (MAMMOTH, TM-align)
463 estimates the degree of superposition of the residue between two structures.

464 The differences (delta) between the scores determined from each modelling path (with the reference set
465 or the negative set) were calculated and used for the PCM machine learning program (see below).

466 For one given candidate, the PCM whole process took an average of 8 CPU-hours (30 minutes on 16
467 CPUs).

468

469 **Taxonomic assignation**

470 pdARDs were taxonomically assigned by combining the results obtained from BLASTN against the NCBI
471 Genomes database (minimal 70% identity and 80% coverage), a BLASTN against the IMOMI in-house
472 database (minimal 85% identity and 90% coverage) and the taxonomy of the metagenomic unit
473 whenever applicable. The lowest taxonomic rank from the results of the three methods was assigned to
474 the pdARD.

475

476 **Statistical analysis**

477 To discriminate reference proteins from negative references, we used model quality predictors and
478 alignment scores (inferred from the semi-automatic pipeline described above) and developed a custom
479 pipeline in R (R Core Team, 2013, <http://www.R-project.org>) to perform the classification. The LASSO

480 penalized logistic regression⁵⁵ implemented in LIBLINEAR⁵⁶ was used to compute the classifier. Ten-
481 fold stratified cross validation (re-sampled 100 times to obtain more stable accuracy estimates) was
482 used to partition the data into a training and test sets. The LASSO hyper-parameter was optimized for
483 each model in a nested 5-fold cross-validation on the training dataset using the area under curve (AUC)
484 as the model selection criterion. From the 100 times re-sampled ten-fold cross validation, receiver
485 operating characteristic (ROC) analysis was used to evaluate model performance using the median
486 AUC. Coefficients extracted for each modelling or alignment score were also evaluated for their stability
487 throughout the computed models. The PCM score was the ratio (expressed as a percentage) between
488 the numbers of time a candidate was classified as a reference and the number of bootstraps. Predicted
489 ARDs were candidates with a PCM score $\geq 50\%$ and a TM score given by TM-align ≥ 0.5 ¹⁷. To control
490 how structural modelling brought additional information compared to amino acid sequence alignment
491 only, we built a logistic regression model based on T-coffee alignment score (R glm, ten-fold
492 stratification, re-sampled 100 times). We then compared the two classifiers models used for PCM and
493 for T-coffee alignment based on the reference set (see Supplementary Information).

494

495 **Validation of the method with a functional metagenomic dataset**

496 The performance of PCM was assessed by analysing the data in Forsberg *et al.*, where the ARD content
497 of different North American soils was analysed using functional metagenomics¹⁸. The screening of the
498 clones was performed on aztreonam, chloramphenicol, ciprofloxacin, colistin, cefepime, cefotaxime,
499 ceftazidime, gentamicin, meropenem, penicillin, piperacillin, piperacillin-
500 tazobactam, tetracycline, tigecycline, trimethoprim and trimethoprim-sulfamethoxazole (cotrimoxazole).
501 Here, we collected the nucleotide sequences of the inserts deposited on Genbank (KJ691878–
502 KJ696532). The sequence translation of the open reading frames was performed by Prodigal (using
503 default parameters)⁴². A total of 4,654 insert sequences were collected, in which 12,904 amino acid
504 sequences were predicted. We then searched for ARDs belonging to the relevant ARD families
505 according to the antibiotics used for the screening of the clones: beta-lactamases (all classes), APH,
506 ANT, AAC(2'), AAC(3)-I, AAC(3)-II, AAC(6'), RNA methylases, Tet(M), Tet(X), Qnr, Sul and DfrA, using
507 the Supplementary Table 2 of the Forsberg *et al.* paper. Inserts with no putative ARDs (according to the
508 annotation of the gene) were removed (n=269). Inserts selected on cycloserine (n=868) and
509 chloramphenicol (n=129) were not considered here because they were not included in the 20 ARD

510 families in this work. Fourteen inserts which contained more than one putative ARD that could be
511 identified to confer resistance to the antibiotic used for the screening (e. g.; two beta-lactamases) were
512 not considered in this analysis. An additional 1,658 inserts containing no putative ARDs or a putative
513 ARDs that did not confer resistance to the antibiotic used for selection were discarded and so were 294
514 inserts containing efflux pumps, as these were not considered in this study. The resulting validation set
515 contained 1,423 inserts (with resistance genes) for a total of 3,778 genes. To compare the outcome of
516 PCM with other tools, the results for class B1-B2 and B3 beta-lactamases generated by PCM were
517 merged into one class B beta-lactamases group as other tools do not separately consider the different
518 class B beta-lactamases.

519 In total, 1,390 unique hits were found during the initial screen of PCM, of which 1,374 were predicted as
520 ARDs (Supplementary Table 7). Among the 33 ARDs not included for PCM, 12 were not considered
521 because they were undersized and 10 because they were oversized. No hits for AAC(2'), ANT, Qnr or
522 Sul were found. The mean identity shared with reference ARDs was 37.6% (range 18.8-94.5). Overall,
523 the sensitivity was 96.6%, with no false negative. In comparison, only 8 ARDs would have been identified
524 by a conventional method (combination of Hmsearch, BLASTP and SSearch with both a minimal
525 identity with a reference ARD and coverage over or equal to 80%). Conversely, Resfams¹¹ that was
526 specifically designed to identify ARDs from functional metagenomic datasets showed a similar sensitivity
527 to PCM with the identification of 1,346 ARDs out of 1,423 (94.6% sensitivity).

528

529 **Validation of the method for incomplete genes**

530 The 3.9 million gene catalogue harbours 41.4% of genes that are predicted to be incomplete either on
531 the 5', the 3' or both extremities¹⁹. As the size parameter is crucial for homology modelling, we tested to
532 what extent the prediction of incomplete ARDs by PCM could remain valid. We selected 12 reference
533 class A beta-lactamases (BlaZ, CbIA-1, CepA-29, CfxA2, CfxA6, CTX-M-8, KPC-10, OXY-1, PER-1,
534 SHV-100, TEM-101 and VEB-1) and we then iteratively removed 5% of the amino acid sequence at
535 both edges in order to obtain 16 bi-directionally trimmed candidates (from 100% to 25%) per reference
536 ARD. Candidate genes were chosen to span the diversity of known beta-lactamases, but the main
537 representative beta-lactamase of the subfamily (e.g. TEM-1 for TEM beta-lactamase) was not
538 necessarily chosen. Note that SHV-100 has a slightly longer sequence (13 amino acid duplication) than
539 other SHV. A total of 192 PCM experiments were performed: we observed that the 12 references were

540 correctly predicted as ARDs when at least 40% of the protein remained (i.e. 30% trim from each
541 extremity, Supplementary Figure 4). Thus, we are confident that with the 75% size threshold used in
542 this study (a maximum of 25% removed from one edge), no misclassification due to an incomplete gene
543 would be expected.

544

545 **Gene synthesis**

546 We selected 71 pdARDs from 12 ARD families: 14 from class A beta-lactamases, 8 from class B1-B2
547 beta-lactamases, 7 from class B3 beta-lactamases, 4 from class C beta-lactamases, 2 from class D
548 beta-lactamases, 2 AAC(3)-I, 5 AAC(3)-II, 8 AAC(6'), 3 ANT, 4 APH, 13 Tet(M) and 1 Tet(X)) for gene
549 synthesis and sub-cloning into *Escherichia coli* to test the decrease of susceptibility to antibiotics. For
550 beta-lactamases, a chromogenic test (nitrocefin) was used to detect function. Minimal inhibitory
551 concentrations (MIC) were determined by E-Test strips (bioMérieux, Marcy-l'Etoile, France) in duplicate.
552 A pdARD was considered to have an activity against an antibiotic (tobramycin for AAC(3)-I, AAC(3)-II,
553 AAC(6') and ANT; kanamycin for APH and tetracycline for Tet(M)) when the MIC of the clone was above
554 the MIC of a clone harbouring the plasmid without a synthesized gene or when the colour of the broth
555 containing nitrocefin turned red, in the case of beta-lactamases. We used the plasmid vector pET-22b+
556 (embedding a beta-lactamase – encoding gene) for pdARDs hypothesized to confer resistance to
557 aminoglycosides and the pET-26b (embedding a gene conferring resistance to kanamycin) for the other
558 pdARDs. The selection of the pdARDs for synthesis was performed as follows:

559 - References (n=12): pdARDs which shared a high identity with known ARDs ($\geq 95\%$ amino acid
560 identity and $\geq 80\%$ coverage with a reference ARD).

561 - Good predictions (n=41): pdARDs with the highest degree of confidence for the prediction (PCM
562 score $> 99\%$, Tm score $TmAlign > 0.9$ and $< 70\%$ amino acid identity with a reference ARD).

563 - Fair predictions (n=18): pdARDs with the lowest degree of confidence for the prediction (PCM score
564 $< 80\%$, Tm score $TmAlign < 0.8$ and $< 70\%$ amino acid identity with a reference ARD).

565

566 **Signatures of mobile genetic elements nearby the predictions of ARDs**

567 We searched for mobile genetic elements (MGE) - associated proteins encoded by genes located in the
568 same contigs as pdARDs. The 3.9 million gene catalogue results from a non-redundancy filtering at 95%
569 for the genes¹⁹, but in order to identify the contigs on which pdARDs were identified, we needed to return

570 to the redundant catalogue (*i.e.* the non-dereplicated catalogue of genes) and identified homologs
571 sharing 95% nucleic acid identity with the pdARDs. By doing so, we could identify contigs (n=16,955)
572 carrying at least one pdARD. The mean size of the contigs was 19,711 bp (min 500, max 461,981,
573 median 8,513). In total, the 16,955 contigs contained a total of 908,888 genes after the subtraction of
574 pdARDs. The 908,888 genes were then translated into proteins with Prodigal⁴² and queried for IS
575 elements using BLASTP (query size threshold 150 amino acids, e-value 1E-30, identity threshold 40%)
576 against the ISfinder database⁵⁷. Conjugative elements were queried among the same gene set
577 (n=908,888) with Conjscan⁵⁸, using the default parameters and the filters recommended by the authors
578 (best e-value<0.001 and sequence coverage of at least 50%). Most proteins belonging to the type IV
579 secretion systems (T4SS), which are involved in conjugation, are ubiquitous in that they have numerous
580 homologs. Hence, when searching for conjugation proteins in a 3.9 million protein catalogue, there
581 would be a high risk of false positives. Accordingly, the colocation of hits was deemed crucial. A
582 conjugative T4SS is made from:

- 583 • a protease (VirB4)
- 584 • a second coupling protein protease (t4cp)
- 585 • a relaxase (MOB)
- 586 • a proteic complex (MPF) composed of at least 10 proteins

587 In order to identify a T4SS on a contig, we required presence of at least 1 virB4 hit, a t4cp1 or t4cp2 hit,
588 a MOB hit and a certain number of MPF hits. All hits must co-localize. A MOB element alone can mobilize
589 a neighboring gene (such as an ARD-encoding gene) via other T4SSs. However, in our dataset the
590 short length of contigs led us to adapt those parameters (following the recommendations of the
591 developers of the Conjscan software). Besides the MOB element, we considered that the presence of 2
592 hits from the same family (e.g. T_virB6 and T_virB8, or B_traF and B_traH) or virB4+any hit from another
593 family on the same contig as a pdARD was a strong indication of the presence of mobility associated
594 elements. Integrons were identified using IntegronFinder⁶⁶ on the 16,955 contigs using default
595 parameters.

596 We also searched for pdARDs in metagenomic species pan-genomes (MSPs)²⁶ obtained from the 9.9
597 million intestinal gene catalogue²⁷ using BLASTN with a 95% identity threshold over 90% of the query.
598 We also searched for homologs of pdARDs in Genbank with 97% identity threshold over 90% of the
599 query. We found 820 out of 6095 pdARDs (13.5%) which aligned against 139,413 Genbank entries. We

600 filtered hits corresponding to a virus, a plasmid or a vague taxonomic affiliation by considering the
601 following terms: "uncultured bacterium", "artificial", "unidentified", "uncultured organism", "environmental
602 samples" and "metagenome".

603 **Distribution of the pdARDs in the MetaHIT cohort (n=663 subjects)**

604 pdARDs profiles were obtained from the abundance matrix of the 3.9 million genes as described in
605 Nielsen *et al*¹⁹. The "reads per kilobase per million mapped reads" (RPKM) method was used to
606 normalize the mapping counts. After summing the relative abundances of pdARDs genes belonging to
607 the same family, Dirichlet multinomial mixture models were used to find ARDs clusters (*i.e.* resistotypes)
608 using the Dirichlet Multinomial R package. The same method was applied to detect gut microbiota
609 clusters (*i.e.* enterotypes)⁵⁹. The Laplace criterion was used to define optimal number of clusters as
610 described on oral and faecal microbial dataset⁶⁰. By analogy with the term enterotype, we chose to name
611 a cluster of subjects based on their similarity of their faecal relative abundance of pdARDs a
612 "resistotype". The Chi-squared test was used to assess the associations between resistotypes and
613 enterotypes. Rarefaction analysis at one million reads was done to determine the gene richness per
614 samples. RLQ analysis⁶¹ was conducted to assess the associations between the relative abundances
615 of pdARDs, their characteristics (family, size of the cluster of associated genes [CAG]) and those of
616 subjects (enterotypes, resistotypes, gender, body mass index [BMI], age). Of note, we excluded the
617 patients suffering from inflammatory bowel disorders from this analysis. Co-inertia analysis was
618 conducted to assess the associations between microbiota beta-diversity and pdARDs profiles.
619 Microbiota composition was assessed using metagenomics species (MGS, see below) relative
620 abundance and beta-diversity by square root Jensen-Shannon Divergence (JSD). A principal coordinate
621 analysis was done on JSD distance matrix and a principal component analysis was done on ARDs
622 profiles. Both analyses were then subjected to co-inertia analysis and Monte-Carlo permutation was
623 done to assess the robustness of shared inertia.

624

625 **Constitution of cohorts of patients with various antibiotic exposures**

626 We included three cohorts of patients with various exposures to antibiotics:

627 - Hospitalization without antibiotics: a total of 31 patients with no exposure to antibiotics or hospitalisation
628 during the three preceding months and admitted to the medicine ward of the Beaujon University

629 Teaching Hospital (Clichy, France) were included and provided a faecal sample at admission. Among
630 them, 16 also provided a stool sample at discharge. One patient received antibiotics between admission
631 and discharge and was not further considered for the analysis. In total, 15 patients could provide a stool
632 sample soon after admission (T0) and at discharge (T1). The mean time between T0 and T1 samples
633 was 10.7 days. The mean age of patients was 67.8 years old and the gender ratio (M/F) was 1.3. All
634 patients gave informed consent. This work was approved by the French National Institutional Review
635 Board (IRB 00008522) and registered at clinicaltrials.gov (NCT02031588).

636 - Chronic exposure: 30 cystic fibrosis (CF) patients were enrolled at the Cystic Fibrosis Unit of the
637 Ramón y Cajal Hospital in Madrid. One faecal sample was collected at the occasion of a consultation.
638 All subjects for this study were provided a consent form describing the study and providing sufficient
639 information for subjects to make an informed decision about their participation as faecal donors in this
640 study. Cystic fibrosis is a genetic disease that leads to an impairment of the lung function through an
641 uncontrolled production of mucus. The consequence is chronic bacterial colonization, resulting in
642 deleterious reactive fibrosis of the lung. Bacterial load is controlled by chronic exposure to antibiotics
643 (home-therapy, mostly oral and inhaled in our cohort), which has resulted in significant life prolongation,
644 and the near-absence of hospital care. Hence, the CF patients had been exposed to various antibiotics
645 during the five years before the faecal sample was collected:

- 646 ▪ Beta-lactams (ampicillin, amoxicillin, cloxacillin, piperacillin-tazobactam, cefepime, ceftriaxone,
647 ceftazidime, ceftiofen, meropenem): 25/30
- 648 ▪ Macrolides (azithromycin, clarithromycin): 17/30
- 649 ▪ Colistin: 21/30
- 650 ▪ Fluoroquinolones (ciprofloxacin, levofloxacin, moxifloxacin): 26/30
- 651 ▪ Cotrimoxazole: 14/30
- 652 ▪ Glycopeptides (vancomycin): 1/30
- 653 ▪ Aminoglycosides (amikacin, tobramycin): 12/30
- 654 ▪ Tetracyclines (doxycycline, minocycline): 2/30
- 655 ▪ Linezolid: 3/30
- 656 ▪ Rifampin: 1/30
- 657 ▪ Fosfomicin: 5/30

658 On average, CF patients had been exposed to 5.9 different antibiotics and had an average of 12.2
659 antibiotic courses during the five years before the sample was taken. The mean age was 36.3 years old
660 and the gender ratio (M/F) was 1.3. This protocol and any amendments were submitted to the Ethics
661 Committee (EC) in agreement with local legal prescriptions, for formal approval of the study conduct.
662 The consent form was obtained before that subject provided any faecal sample for the study and was
663 signed by the subject or legally acceptable surrogate, and the investigator-designated research
664 professional obtaining the consent. According to the National Spanish laws the study did not require the
665 approval of the Ethics Committee. Nonetheless, the Ethics Committee of the Hospital Ramón y Cajal
666 guaranteed that the study was performed done according to the good clinical practices guidelines.

667 - Short high dose exposure: selective digestive decontamination (SDD) consists in administering a
668 mixture of topical and parenteral antibiotics and antifungal agents to a patient at admission in order to
669 eliminate potential bacterial and fungal pathogens. SDD has been showed to significantly reduce
670 mortality in the intensive care unit (ICU)²⁹ and is now part of standard care for intensive care patients in
671 the Netherlands. To assess the effect of SDD on the intestinal microbiota, we analysed the faecal
672 samples from 13 patients admitted to the ICU of the University Medical Centre of Utrecht (UMCU,
673 Netherlands). The samples were collected at admission (T0, first sample passed after admission) and
674 after SDD (T1). Among the 13 patients for whom a faecal sample could be obtained at T0, 10 could
675 provide a faecal sample at T1. The mean age was 59.9 years old and the gender ratio (M/F) was 0.5.
676 SDD consisted of 4 days of intravenous cefotaxime and topical application of tobramycin, colistin, and
677 amphotericin B. Additionally, a subset of samples (n=4) from this cohort was cultured in a brain-heart
678 infusion broth overnight in ambient atmosphere at 37°C. The protocol for the collection of stool samples
679 was reviewed and approved by the institutional review board of the University Medical Centre of Utrecht
680 (The Netherlands) under number 10/0225. Informed consent for faecal sampling during hospitalization
681 was waived. Written consent was obtained for the collection of faecal samples after hospitalization.

682

683 **Metagenomic sequencing and mapping.**

684 Total faecal DNA was extracted^{62,63} and sequenced using SOLiD 5500 wildfire (Life Technologies)
685 resulting in a mean of 68.5 million sequences of 35-base-long single-end reads. High-quality reads were
686 generated with quality score cut-off >20. Reads with a positive match with human, plant, cow or SOLiD
687 adapter sequences were removed.

688 Filtered high-quality reads were mapped to the MetaHIT 3.9 million gene catalogue¹⁹ using the METEOR
689 software⁶⁴. The read alignments were performed in colour-space with Bowtie software (version 1.1.0)⁶⁵.
690 Uniquely mapped reads (reads mapping to a single gene from the catalogue) were attributed to the
691 corresponding genes. Shared reads (mapping different genes of the catalogue) were attributed
692 according to the ratio of their unique mapping counts, as following: as a read can map on different genes
693 of the catalogue, the abundance of a gene $G(A_g)$ depends on the abundance of uniquely mapped reads
694 (A_u), *i.e.* reads that map only to the gene G , and on the abundance of N shared reads (A_s) that aligned
695 with M genes in addition to the gene G :

$$A_g = A_u + A_s$$

697 where

$$A_s = \sum_{i=1}^M C_{o_i}$$

699
700 For each shared read, the gain of abundance corresponds to a coefficient C_o that takes in account the
701 total number of uniquely mapped reads on the M genes:

$$C_{o_i} = \frac{A_u}{A_u + \sum_{j=1}^M A_{u_j}}$$

703
704 For instance, if a gene G is mapped by 10 reads that only map to it (unique reads), but also with 1 read
705 that also align on a gene M that was mapped by 5 unique reads, then:

$$A_g = 10 + \frac{10}{10 + 5} \approx 10.7$$

707
708 To decrease technical biases due to different sequencing depth, samples with at least 5 million mapped
709 reads were downsized to 5 million mapped reads (random sampling of 5 million mapped reads without
710 replacement) using R package momr³¹. The abundance of each gene in a sample was then normalized
711 by dividing the number of reads that mapped to the gene (A_g) by the gene nucleotide length and by the
712 total number of reads from the sample. The resulting set of gene abundances, termed a “microbial gene
713 profile”, was used to estimate the abundance of metagenomic species (MGS)¹⁹.

714
715 *Gene richness analysis*

716 Microbial gene richness was calculated by counting the number of genes mapped at least once for a
717 given sample. Gene richness was calculated using R package momr for samples where 5 million or
718 more reads had been mapped to the 3.9 million gene catalogue.

719

720 *MetaGenomic Species (MGS)*

721 MGS are co-abundance gene groups with more than 700 genes and can be considered as part of
722 complete bacterial species genomes. 741 MGS were delineated from 396 human gut microbiome
723 samples¹⁹. In this study, the relative abundance of MGS was determined as the median abundance of
724 90% of the genes composing each cluster, meaning that the 10% genes with the lowest abundance for
725 each MGS were not considered for the calculation of the abundance of the MGS. Typically, these genes
726 correspond to genes with 0 count, to accessory genes (hence their detection is not constant) or to genes
727 that are not detected because of insufficient sequencing depth. The MGS taxonomical annotation was
728 updated by sequence similarity using NCBI BLASTN, when more than 50% of the genes matched the
729 same reference of NCBI database (December 2014 version) at a threshold of 95% of identity and 90%
730 of gene length coverage to get the species annotation¹⁹.

731

732 *Statistical analysis for the distribution of pdARDs and MGS between groups*

733 Statistical analyses for the differential abundances of pdARDs and MGS were performed using the
734 application SHAMAN⁶⁶ (<http://shaman.c3bi.pasteur.fr/>). Data are available at
735 (<https://github.com/aghozlane/evotar>), with the graphical representations using the abundances from
736 the matrix rarefied at 5M reads. The relationship between richness and the abundance of ARDs was
737 assessed by Spearman correlation test. The statistical threshold for significance was set at a p-value of
738 0.05.

739

740 *Data availability*

741 The 6,095 pdARDs PDB files, nucleotide and amino acid sequences can be downloaded from
742 <http://mgps.eu/Mustard/>. The 3.9 million gene catalogue and the metagenomic species database are
743 accessible at <https://www.cbs.dtu.dk/projects/CAG/>. The reads from the clinical samples generated in
744 this study are available under the accession number PRJEB27799 at the European Nucleotide Archive
745 (ENA).

746

747 *Code availability*

748 The PCM code can be found at <https://github.com/aghozlane/pcm>.

749

750 **References**

751

752 1. Qin, J. *et al.* A human gut microbial gene catalogue established by metagenomic sequencing.

753 *Nature* **464**, 59–65 (2010).

754 2. Ghosh, T. S., Gupta, S. S., Nair, G. B. & Mande, S. S. In silico analysis of antibiotic resistance

755 genes in the gut microflora of individuals from diverse geographies and age-groups. *PLoS One* **8**,

756 e83823 (2013).

757 3. Hu, Y. *et al.* Metagenome-wide analysis of antibiotic resistance genes in a large cohort of human

758 gut microbiota. *Nat. Commun.* **4**, 2151 (2013).

759 4. Forslund, K. *et al.* Country-specific antibiotic use practices impact the human gut resistome.

760 *Genome Res.* **23**, 1163–1169 (2013).

761 5. Sommer, M. O. A., Dantas, G. & Church, G. M. Functional characterization of the antibiotic

762 resistance reservoir in the human microflora. *Science* **325**, 1128–1131 (2009).

763 6. Moore, A. M. *et al.* Pediatric fecal microbiota harbor diverse and novel antibiotic resistance genes.

764 *PLoS One* **8**, e78822 (2013).

765 7. Gupta, S. K. *et al.* ARG-ANNOT, a new bioinformatic tool to discover antibiotic resistance genes

766 in bacterial genomes. *Antimicrob. Agents Chemother.* **58**, 212–220 (2014).

767 8. McArthur, A. G. *et al.* The comprehensive antibiotic resistance database. *Antimicrob. Agents*

768 *Chemother.* **57**, 3348–3357 (2013).

769 9. Zankari, E. *et al.* Identification of acquired antimicrobial resistance genes. *J. Antimicrob.*

770 *Chemother.* **67**, 2640–2644 (2012).

771 10. Arango-Argoty, G. *et al.* DeepARG: a deep learning approach for predicting antibiotic resistance

772 genes from metagenomic data. *Microbiome* **6**, 23 (2018).

773 11. Gibson, M. K., Forsberg, K. J. & Dantas, G. Improved annotation of antibiotic resistance

774 determinants reveals microbial resistomes cluster by ecology. *ISME J.* **9**, 207–216 (2015).

- 775 12. Wright, G. D. The antibiotic resistome: the nexus of chemical and genetic diversity. *Nat. Rev.*
776 *Microbiol.* **5**, 175–186 (2007).
- 777 13. Salyers, A. A., Gupta, A. & Wang, Y. Human intestinal bacteria as reservoirs for antibiotic
778 resistance genes. *Trends Microbiol.* **12**, 412–416 (2004).
- 779 14. Ghosh, S., Sadowsky, M. J., Roberts, M. C., Gralnick, J. A. & LaPara, T. M. *Sphingobacterium* sp.
780 strain PM2-P1-29 harbours a functional tet(X) gene encoding for the degradation of tetracycline. *J.*
781 *Appl. Microbiol.* **106**, 1336–1342 (2009).
- 782 15. Stinear, T. P., Olden, D. C., Johnson, P. D., Davies, J. K. & Grayson, M. L. Enterococcal vanB
783 resistance locus in anaerobic bacteria in human faeces. *Lancet* **357**, 855–856 (2001).
- 784 16. Penders, J., Stobberingh, E. E., Savelkoul, P. H. M. & Wolffs, P. F. G. The human microbiome as
785 a reservoir of antimicrobial resistance. *Front. Microbiol.* **4**, (2013).
- 786 17. Zhang, Y. & Skolnick, J. TM-align: a protein structure alignment algorithm based on the TM-score.
787 *Nucleic Acids Res.* **33**, 2302–2309 (2005).
- 788 18. Forsberg, K. J. *et al.* Bacterial phylogeny structures soil resistomes across habitats. *Nature* **509**,
789 612–616 (2014).
- 790 19. Nielsen, H. B. *et al.* Identification and assembly of genomes and genetic elements in complex
791 metagenomic samples without using reference genomes. *Nat. Biotechnol.* **32**, 822–828 (2014).
- 792 20. Goossens, H., Ferech, M., Vander Stichele, R., Elseviers, M. & ESAC Project Group. Outpatient
793 antibiotic use in Europe and association with resistance: a cross-national database study. *Lancet*
794 **365**, 579–587 (2005).
- 795 21. Altschul, S. F., Gish, W., Miller, W., Myers, E. W. & Lipman, D. J. Basic local alignment search
796 tool. *J. Mol. Biol.* **215**, 403–410 (1990).
- 797 22. Berglund, F. *et al.* Identification of 76 novel B1 metallo- β -lactamases through large-scale
798 screening of genomic and metagenomic data. *Microbiome* **5**, (2017).
- 799 23. Everard, A. *et al.* Cross-talk between *Akkermansia muciniphila* and intestinal epithelium controls
800 diet-induced obesity. *Proc. Natl. Acad. Sci. U. S. A.* **110**, 9066–9071 (2013).
- 801 24. Sokol, H. *et al.* *Faecalibacterium prausnitzii* is an anti-inflammatory commensal bacterium
802 identified by gut microbiota analysis of Crohn disease patients. *Proc. Natl. Acad. Sci. U. S. A.* **105**,
803 16731–16736 (2008).

- 804 25. Leski, T. A. *et al.* Multidrug-resistant tet(X)-containing hospital isolates in Sierra Leone. *Int. J.*
805 *Antimicrob. Agents* **42**, 83–86 (2013).
- 806 26. Oñate, F. P. *et al.* MSPminer: abundance-based reconstitution of microbial pan-genomes from
807 shotgun metagenomic data. *bioRxiv* 173203 (2018). doi:10.1101/173203
- 808 27. Li, J. *et al.* An integrated catalog of reference genes in the human gut microbiome. *Nat.*
809 *Biotechnol.* **32**, 834–841 (2014).
- 810 28. Arumugam, M. *et al.* Enterotypes of the human gut microbiome. *Nature* **473**, 174–180 (2011).
- 811 29. de Smet, A. M. G. A. *et al.* Decontamination of the digestive tract and oropharynx in ICU patients.
812 *N. Engl. J. Med.* **360**, 20–31 (2009).
- 813 30. van Schaik, W. The human gut resistome. *Philos. Trans. R. Soc. Lond. B. Biol. Sci.* **370**, (2015).
- 814 31. Le Chatelier, E. *et al.* Richness of human gut microbiome correlates with metabolic markers.
815 *Nature* **500**, 541–546 (2013).
- 816 32. Pehrsson, E. C. *et al.* Interconnected microbiomes and resistomes in low-income human habitats.
817 *Nature* **533**, 212–216 (2016).
- 818 33. Léonard, F., Andremont, A., Leclercq, B., Labia, R. & Tancrede, C. Use of beta-lactamase-
819 producing anaerobes to prevent ceftriaxone from degrading intestinal resistance to colonization. *J.*
820 *Infect. Dis.* **160**, 274–280 (1989).
- 821 34. Bilinski, J. *et al.* Fecal Microbiota Transplantation in Patients with Blood Disorders Inhibits Gut
822 Colonization with Antibiotic-Resistant Bacteria: Results of a Prospective, Single-Center Study.
823 *Clin. Infect. Dis.* (2017). doi:10.1093/cid/cix252
- 824 35. Lupo, A., Coyne, S. & Berendonk, T. U. Origin and Evolution of Antibiotic Resistance: The
825 Common Mechanisms of Emergence and Spread in Water Bodies. *Front. Microbiol.* **3**, (2012).
- 826 36. Lagier, J.-C. *et al.* Culture of previously uncultured members of the human gut microbiota by
827 culturomics. *Nat. Microbiol.* **1**, 16203 (2016).
- 828 37. Illergård, K., Ardell, D. H. & Elofsson, A. Structure is three to ten times more conserved than
829 sequence--a study of structural response in protein cores. *Proteins* **77**, 499–508 (2009).
- 830 38. Baquero, F., Tedim, A. P. & Coque, T. M. Antibiotic resistance shaping multi-level population
831 biology of bacteria. *Front. Microbiol.* **4**, 15 (2013).
- 832 39. Martínez, J. L., Coque, T. M. & Baquero, F. What is a resistance gene? Ranking risk in
833 resistomes. *Nat. Rev. Microbiol.* **13**, 116–123 (2015).

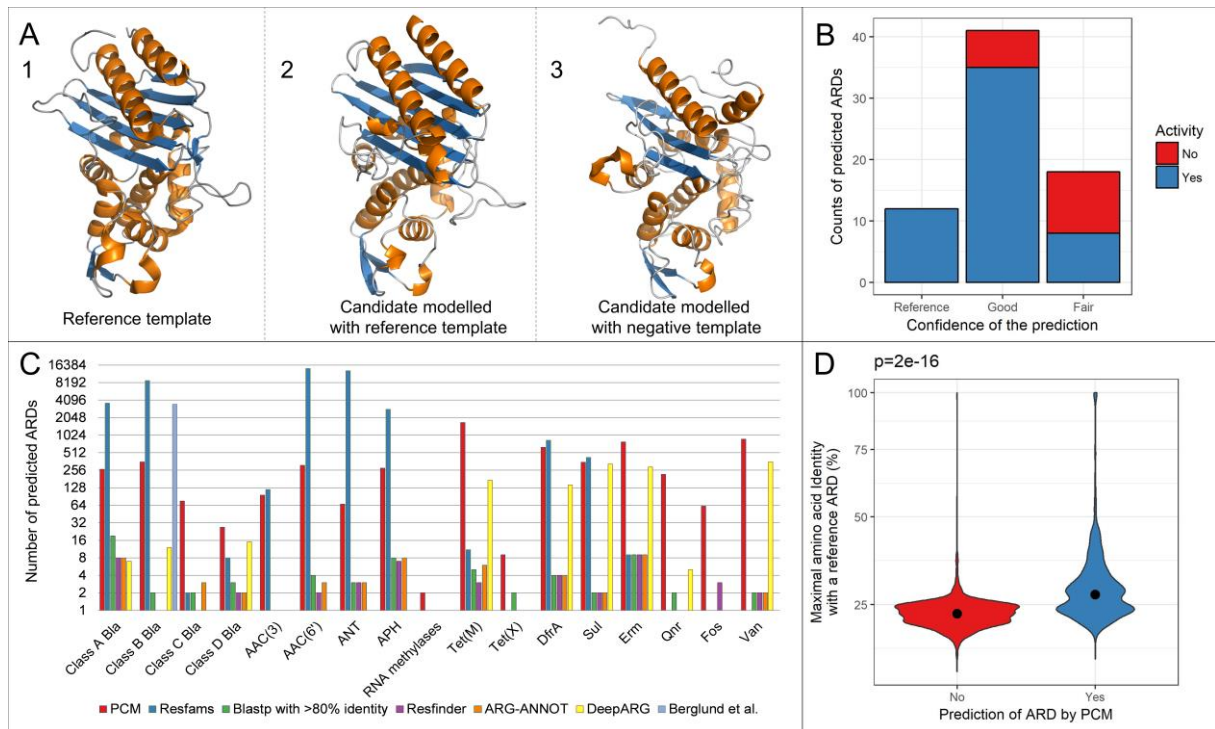
- 834 40. Van Boeckel, T. P. *et al.* Global antibiotic consumption 2000 to 2010: an analysis of national
835 pharmaceutical sales data. *Lancet Infect. Dis.* **14**, 742–750 (2014).
- 836 41. Allen, H. K., Moe, L. A., Rodbumrer, J., Gaarder, A. & Handelsman, J. Functional metagenomics
837 reveals diverse beta-lactamases in a remote Alaskan soil. *ISME J.* **3**, 243–251 (2009).
- 838 42. Hyatt, D. *et al.* Prodigal: prokaryotic gene recognition and translation initiation site identification.
839 *BMC Bioinformatics* **11**, 119 (2010).
- 840 43. Fu, L., Niu, B., Zhu, Z., Wu, S. & Li, W. CD-HIT: accelerated for clustering the next-generation
841 sequencing data. *Bioinformatics* **28**, 3150–3152 (2012).
- 842 44. Powell, S. *et al.* eggNOG v3.0: orthologous groups covering 1133 organisms at 41 different
843 taxonomic ranges. *Nucleic Acids Res.* **40**, D284-289 (2012).
- 844 45. Liu, Y.-Y. *et al.* Emergence of plasmid-mediated colistin resistance mechanism MCR-1 in animals
845 and human beings in China: a microbiological and molecular biological study. *Lancet Infect. Dis.*
846 **16**, 161–168 (2016).
- 847 46. Finn, R. D., Clements, J. & Eddy, S. R. HMMER web server: interactive sequence similarity
848 searching. *Nucleic Acids Res.* **39**, W29-37 (2011).
- 849 47. Pearson, W. R. & Lipman, D. J. Improved tools for biological sequence comparison. *Proc. Natl.*
850 *Acad. Sci. U. S. A.* **85**, 2444–2448 (1988).
- 851 48. Berman, H. M. *et al.* The Protein Data Bank. *Nucleic Acids Res.* **28**, 235–242 (2000).
- 852 49. Sievers, F. *et al.* Fast, scalable generation of high-quality protein multiple sequence alignments
853 using Clustal Omega. *Mol. Syst. Biol.* **7**, 539 (2011).
- 854 50. Jones, D. T. Protein secondary structure prediction based on position-specific scoring matrices. *J.*
855 *Mol. Biol.* **292**, 195–202 (1999).
- 856 51. Sali, A. & Blundell, T. L. Comparative protein modelling by satisfaction of spatial restraints. *J. Mol.*
857 *Biol.* **234**, 779–815 (1993).
- 858 52. Wallner, B. & Elofsson, A. Can correct protein models be identified? *Protein Sci. Publ. Protein*
859 *Soc.* **12**, 1073–1086 (2003).
- 860 53. Wiederstein, M. & Sippl, M. J. ProSA-web: interactive web service for the recognition of errors in
861 three-dimensional structures of proteins. *Nucleic Acids Res.* **35**, W407-410 (2007).

- 862 54. Ortiz, A. R., Strauss, C. E. M. & Olmea, O. MAMMOTH (matching molecular models obtained
863 from theory): an automated method for model comparison. *Protein Sci. Publ. Protein Soc.* **11**,
864 2606–2621 (2002).
- 865 55. Tibshirani, R. Regression shrinkage and selection via the lasso. *J R. Stat. Soc B* **58**, 267–288
866 (1996).
- 867 56. Fan, R. E., Chang, K. W., Hsieh, C. J., Wang, X. R. & Lin, C. J. A library for large linear
868 classification. *JMLR* **9**, 1871–1874
- 869 57. Siguier, P., Perochon, J., Lestrade, L., Mahillon, J. & Chandler, M. ISfinder: the reference centre
870 for bacterial insertion sequences. *Nucleic Acids Res.* **34**, D32-36 (2006).
- 871 58. Guglielmini, J., Quintais, L., Garcillán-Barcia, M. P., de la Cruz, F. & Rocha, E. P. C. The
872 repertoire of ICE in prokaryotes underscores the unity, diversity, and ubiquity of conjugation. *PLoS*
873 *Genet.* **7**, e1002222 (2011).
- 874 59. Holmes, I., Harris, K. & Quince, C. Dirichlet multinomial mixtures: generative models for microbial
875 metagenomics. *PloS One* **7**, e30126 (2012).
- 876 60. Ding, T. & Schloss, P. D. Dynamics and associations of microbial community types across the
877 human body. *Nature* **509**, 357–360 (2014).
- 878 61. Dray, S. & Legendre, P. Testing the species traits-environment relationships: the fourth-corner
879 problem revisited. *Ecology* **89**, 3400–3412 (2008).
- 880 62. Godon, J. J., Zumstein, E., Dabert, P., Habouzit, F. & Moletta, R. Molecular microbial diversity of
881 an anaerobic digester as determined by small-subunit rDNA sequence analysis. *Appl. Environ.*
882 *Microbiol.* **63**, 2802–2813 (1997).
- 883 63. Suau, A. *et al.* Direct analysis of genes encoding 16S rRNA from complex communities reveals
884 many novel molecular species within the human gut. *Appl. Environ. Microbiol.* **65**, 4799–4807
885 (1999).
- 886 64. Pons, N. *et al.* METEOR - a platform for quantitative metagenomic profiling of complex
887 ecosystems. in (2010).
- 888 65. Langmead, B. & Salzberg, S. L. Fast gapped-read alignment with Bowtie 2. *Nat. Methods* **9**, 357–
889 359 (2012).
- 890 66. Quereda, J. J. *et al.* Bacteriocin from epidemic *Listeria* strains alters the host intestinal microbiota
891 to favor infection. *Proc. Natl. Acad. Sci. U. S. A.* **113**, 5706–5711 (2016).

892 67. Robert, P. & Escoufier, Y. A Unifying Tool for Linear Multivariate Statistical Methods: The RV-
893 Coefficient. *Appl. Stat.* **25**, 257 (1976).
894

895 **Figures**

896 **Figure 1:** Illustration of the concept of “Pairwise Comparative Modelling” (PCM) with a class A beta-
897 lactamase (panel A). A1: class A beta-lactamase protein structure (4EWF) obtained from the PDB
898 database. A2: A candidate protein (MC3.MG12.AS1.GP1.C14.G3 from *Faecalibacterium prausnitzii*) for
899 class A beta-lactamase modelled with a reference class A beta-lactamase structural template. This
900 protein had 26.5% amino acid identity with the closest reference class A beta-lactamase. A3: The same
901 candidate protein (MC3.MG12.AS1.GP1.C14.G3) for class A beta-lactamase this time modelled with a
902 negative reference template. The candidate MC3.MG12.AS1.GP1.C14.G3 was predicted to be a class
903 A beta-lactamase with 100% confidence by our model and later found to be functional after gene
904 synthesis. Panel B: Bar-plot of the activity of the synthesized pdARDs against antibiotics with respect to
905 the degree of confidence of the prediction (“reference” meaning that the protein shares more $\geq 95\%$
906 amino acid identity with a functionally proven ARD, “good” meaning a PCM score over 99% and a
907 TmAlign Tm score ≥ 0.8 , “fair” meaning a PCM score between 50% and 80%). Panel C: number of
908 predictions of antibiotic resistance determinants from a 3.9 million gene catalogue of the intestinal
909 microbiota¹⁹ using PCM, BLASTP²¹, ARG-ANNOT⁷, Resfinder⁹, DeepARG¹⁰, Resfams¹¹ and the HMM-
910 based method published by Berglund *et al.* for class B1 beta-lactamases²². Panel D: violin plot of the
911 maximal identity observed with a reference ARD for candidates predicted as ARDs (blue violin, n=6,095)
912 and those not predicted as ARDs (red violin, n=3,982). The point depicts the median. The width of the
913 violins depicts the distribution of pdARDs according to their maximal identity with a reference ARD. See
914 Supplementary Table 2 for details about candidates sharing at least 40% identity with reference ARDs
915 but which were not predicted as ARDs.

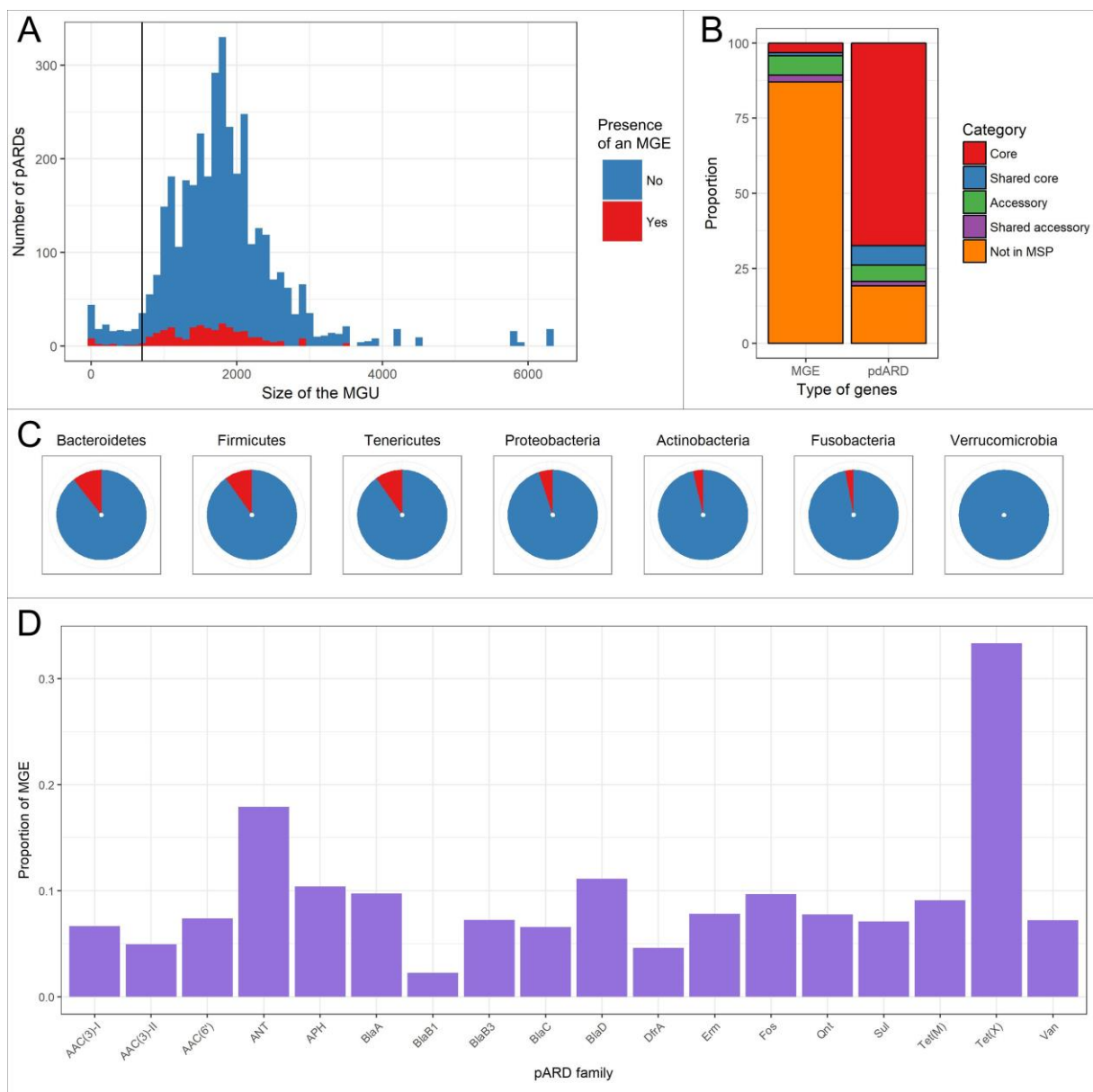


916

917 Bla: beta-lactamase; AAC: aminoglycoside acetylase; ANT: aminoglycoside nucleotidyl transferase;
 918 APH: aminoglycoside phosphotransferase; DfrA: type A dihydrofolate reductase; Sul: dihydropteroate
 919 synthase; Erm: erythromycin ribosome methylase; Qnr: quinolone resistance; Fos: fosfomycin
 920 resistance (Fos); Van: D-Ala – D-Lac/Ser ligase (vancomycin resistance).

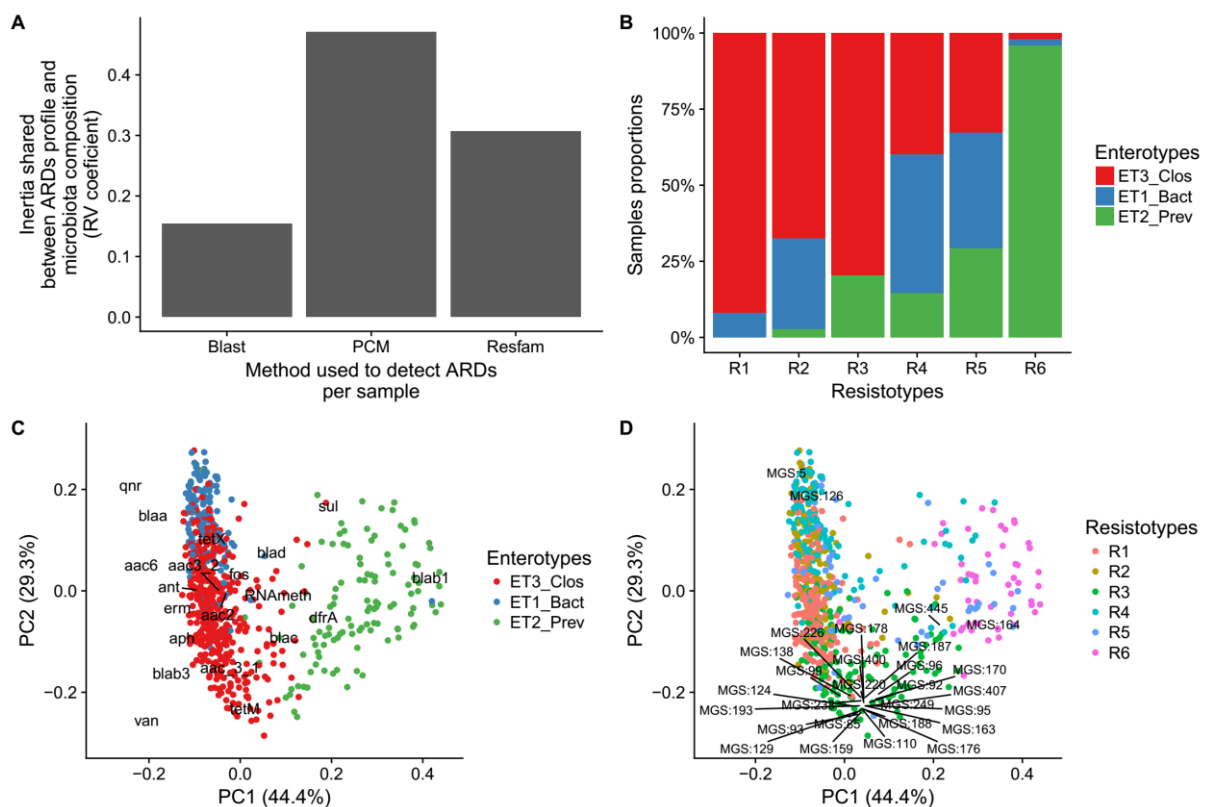
921

922 **Figure 2:** Mobile genetic elements (MGE) and predicted antibiotic resistance determinants (pdARDs).
 923 (A) Distribution of the sizes of the metagenomics unit (MGU) where an antibiotic resistance determinant
 924 was predicted with respect to the colocation of MGE-associated genes. The vertical line depicts the
 925 assumed gene size threshold above which MGUs are considered as partial chromosomes referred as
 926 metagenomic species (MGS)¹⁹. (B) Bar plot of the categories of metagenomic species pangenomes
 927 (MSPs)²⁶ assigned to MGE – associated genes²⁷ and pdARDs. (C) Proportion of pdARDs co-locating
 928 with MGE-associated genes with respect to their phylum. (D) Proportion of pdARDs co-locating with
 929 MGE-associated genes according to the pdARD family. Of note, the AAC(2') and 16S RNA methylases
 930 only included 3 and 2 pdARDs, respectively and were accordingly not depicted in this panel.



931

932 **Figure 3:** Association between resistotypes, enterotypes, metagenomics species (MGS) and pdARDs
 933 profiles in the 663 individuals from the MetaHIT cohort. A) inertia shared between pdARDs profiles and
 934 microbiota composition as function of bioinformatics methods. We assessed how gut microbiota beta
 935 diversity inertia was connected to the abundance of pdARDs. Co-inertia using RV coefficient was
 936 analysed to detect significant co-structure between datasets⁶⁷, meaning that different sets of variables
 937 (e.g. microbial genera abundance and ARDs profiles) were not independent and shared a fraction of
 938 inertia. Monte- Carlo tests were used to confirm observed relations between different datasets,
 939 assuming a p-value < 0.05. B) Samples proportions for each resistotype depicted as function of
 940 enterotypes using the PCM method. C) and D) Association between pdARDs gene profile and gut
 941 microbiota composition using co-inertia analysis with respect to their enterotypes and pdARDs families
 942 (C), and to their resistotypes and MGS relative abundance (D). A taxonomical correspondence for each
 943 MGS number can be found in the original paper¹⁹. Briefly, all MGS were Firmicutes with the exception
 944 of MGS:164 and MGS:445 (both Bacteroidetes).

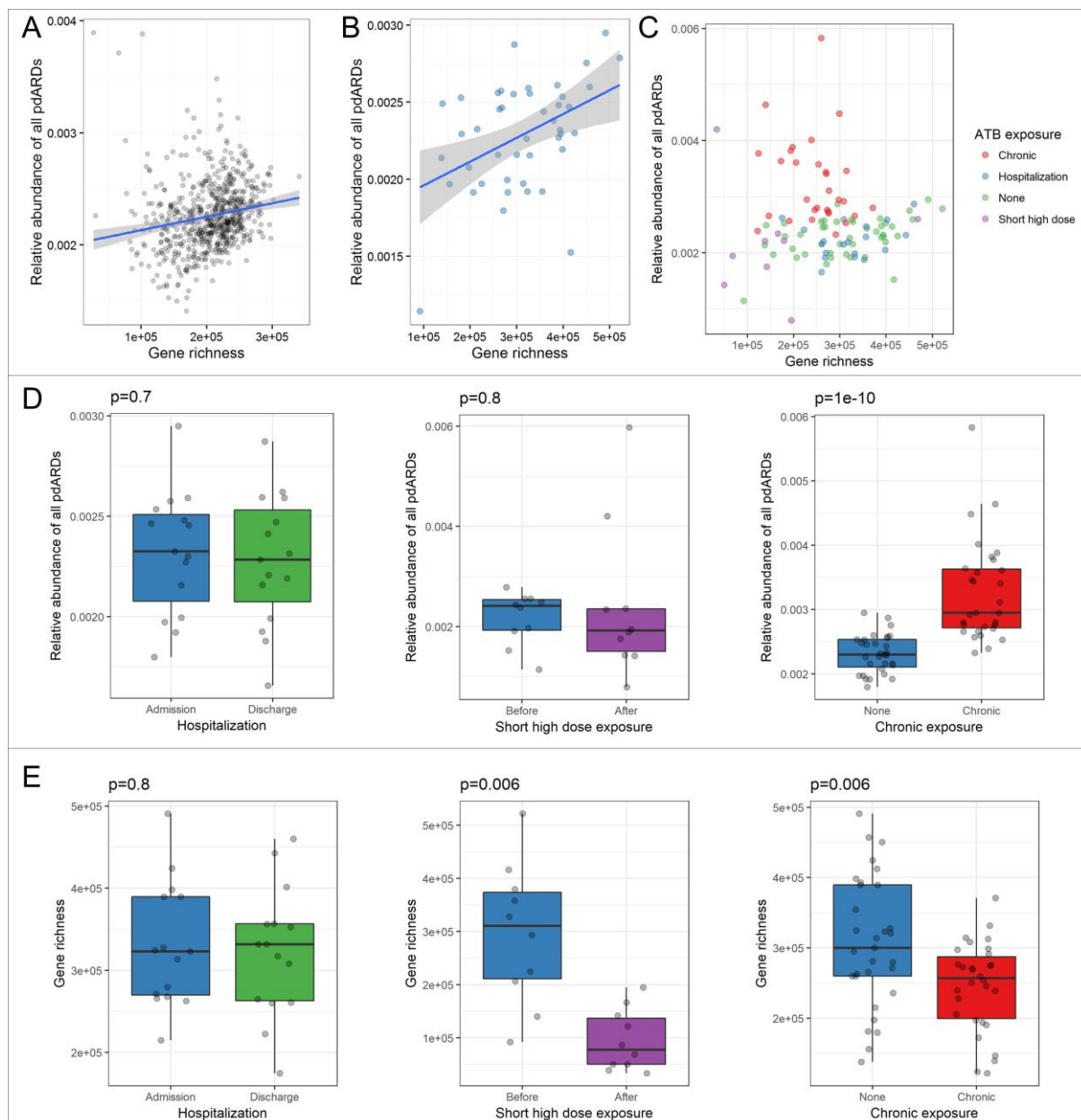


945

946

947

948 **Figure 4:** (A) Gene richness and relative abundance of predicted antibiotic resistance determinants
 949 (pdARDs) in the MetaHIT cohort (n=663). (B) Gene richness and relative abundance of pdARDs in our
 950 cohort of subjects with no recent antibiotic exposure (n=44). (C) Gene richness and relative abundance
 951 of pdARDs in our cohort of subjects with regards to their antibiotic exposure (n=102 samples). (D) and
 952 (E) Boxplots superimposed by dot plots of the comparisons of the relative abundance of all pdARDs and
 953 gene richness, respectively, between the various groups differing by their exposure to antibiotics.
 954 Hospitalization: n=15, Wilcoxon paired test. Short high dose exposure: n=10, Wilcoxon paired test.
 955 Chronic exposure: n=31 for patients not exposed to antibiotics, n=30 for patients chronically exposed to
 956 antibiotics, Wilcoxon unpaired test.



957

958 ATB: antibiotics. The shaded grey area depicts the 95% confidence interval around the blue, linear
959 regression line. For boxplots, the lower, central and upper hinges correspond to the first, second
960 (median) and third quartiles. The upper and lower whiskers respectively correspond to the higher and
961 lower values at $1.5 \cdot \text{IQR}$ from the hinge (where IQR is the inter-quartile range, or distance between the
962 first and third quartiles).

963 **Table 1:** Summary of the predictions of antibiotic resistance determinants (ARDs) from a 3.9 million
 964 gene catalogue of the intestinal microbiota¹⁹ and of gene synthesis results.

Antibiotic resistance class	Number of references	Number of candidates	Number of predictions	Rate ARD predictions/candidates (%)	Tested (%)	N functional (%)	N not functional (%)
16S rRNA methylase	17	4	2	50,0	0 (0%)	NA	NA
AAC(2')	5	15	3	20,0	0 (0%)	NA	NA
AAC(3)-I	7	53	15	28,3	2 (13.3%)	2 (100%)	0 (0%)
AAC(3)-II	12	81	81	100	5 (6.2%)	5 (100%)	0 (0%)
AAC(6')	36	1191	312	26,2	8 (2.6%)	6 (75%)	2 (25%)
ANT	29	158	67	42,4	3 (4.5%)	3 (100%)	0 (0%)
APH	30	430	279	64,9	4 (1.4%)	3 (75%)	1 (25%)
Class A beta-lactamase	682	402	267	66,4	14 (5.2%)	9 (64.3%)	5 (35.7%)
Class B1-B2 beta-lactamase	150	554	134	24,2	8 (6.0%)	6 (75%)	2 (25%)
Class B3 beta-lactamase	31	493	221	44,8	7 (3.2%)	5 (71.4%)	2 (28.6%)
Class C beta-lactamase	56	373	76	20,4	4 (5.3%)	4 (100%)	0 (0%)
Class D beta-lactamase	248	76	27	35,5	2 (7.4%)	2 (100%)	0 (0%)
DfrA	35	632	632	100	0 (0%)	NA	NA
Erm	58	873	781	89,5	0 (0%)	NA	NA
Fos	34	84	62	73,8	0 (0%)	NA	NA
Qnr	66	272	219	80,5	0 (0%)	NA	NA
Sul	33	357	353	98,9	0 (0%)	NA	NA
Tet(M)	72	2824	1682	59,6	13 (0.8%)	9 (69.2%)	4 (30.8%)
Tet(X)	12	42	9	21,4	1 (11.1%)	1 (100%)	0 (0%)
Van ligase	16	1163	873	75,1	0 (0%)	NA	NA

965